Ion−Molecule Chemistry within Boron Tribromide Clusters: Experiment and Theory

David A. Hales,* Kathryn E. Kautzman, Nathan G. Williams, Pamela A. Haile, and Michael P. Barker

Department of Chemistry, Hendrix College, 1600 Washington Avenue, Conway, Arkansas 72032

Received: August 15, 2006; In Final Form: December 22, 2006

Ⓦ **This paper contains enhanced objects available on the Internet at http://pubs.acs.org/jpca.**

Molecular clusters of BBr_3 were subjected to electron ionization and mass analysis in a reflectron time-of-flight mass spectrometer. Five series of cluster ions were observed, with formulas corresponding to each of the possible fragment ions of BBr_3 being solvated by neutral BBr_3 molecules. Geometry optimizations on the observed cluster ions using density functional theory (B3LYP/6-31G*) predict that fragment ions smaller than BBr_3^+ undergo reactions with neutral BBr_3 molecules to form covalently bound adduct species that function as core ions within the clusters. Once all boron atoms are saturated, the reactions cease, and larger cluster ions consist of BBr_3 molecules loosely bound to the core ions. Divalent bromine atoms are present in at least three of the cluster ions, and most of the intermolecular contact within the clusters is between Br atoms. Enthalpies of formation, addition reactions, and BBr_3 elimination from the cluster ions were derived from B3LYP and MP2 calculations at the B3LYP/6-31G* geometries using both the 6-31G* and the 6-311++G(2df,2p) basis sets. The results are compared to limiting expectations based on known bulk thermochemistry.

Introduction

Plasma processing is an important technique in semiconductor manufacturing, and the boron halides play a significant role in such work. The simultaneous presence in a plasma of both charged and neutral species ensures that ion−molecule encounters will occur and raises the plausibility of ion−molecule chemistry taking place in the plasma. Any resulting reactions will affect the composition of the plasma, so an understanding of these reactions will be helpful in understanding and modeling plasma conditions. Polyboron halides (B_nX_m, $n > 1$) are probably not involved to any meaningful degree in the chemistry of the plasma etching process. However, the fact that they have been synthesized from smaller boron halides in discharges raises the question of whether they might be formed, even transiently, in industrial or laboratory plasmas.[1] In spite of all this, relatively little is known about boron halide ion−molecule chemistry.

Several studies have examined reactions of BX_3 with various anions, but less is known about the chemistry of these molecules with positive ions. The literature includes reactions of BX_3 with F_2^+ in studies of the gas-phase basicity of that ion;[2] proton affinity studies with H_3^+ and CH_5^+;[3] and studies of interactions with C_{60}^{2+}, where cage size reduction is seen in the fullerene after it acquires an electron from a BCl_3 molecule.[4] As might be expected from the identities of the reactant cations in these cases, no $B_nX_m^+$ species with $n > 1$ were observed. Formation of $B_nX_m^+$ with $n > 1$ would require BX_n^+ ($n = 1-3$) ions to be present with BX_3, a situation that has been created in two studies with X = Cl. In a study of BCl_3-containing plasma, it was found that no positive ions heavier than BCl_3^+ were formed under their experimental conditions, even though BCl_n^+ ($n = 1-3$) and neutral BCl_3 were present together in the plasma.[5] A study of BCl_3 ion−molecule chemistry by FTMS found that neither BCl^+ nor BCl_2^+ reacted with BCl_3 under isolated collision conditions.[6] These observations do not rule out the possibility that $B_nCl_m^+$ with $n > 1$ might be formed under different conditions. A synchrotron photoionization study of $(BF_3)_n(CH_3OCH_3)_m$ heteroclusters did yield ions with the compositions $[B_2F_5(CH_3OCH_3)_2]^+$ and $[B_2F_5(CH_3OCH_3)_3]^+$, but the possible structures of these ions were not addressed.[7] It seems possible, according to previous work from this laboratory, that these cluster ions might include the $B_2F_5^+$ fragment that was computationally predicted to be ubiquitous in $B_nF_{3n-1}^+$ cluster ions.[8]

Overall, this does not represent a very large or complete body of knowledge of the chemistry of BX_3 with positive ions. In particular, BBr_3 and BI_3 are strongly underrepresented, and very few studies have even detected, much less addressed the properties of, $B_nX_m^+$ with $n > 1$. In this work, we present some aspects of BBr_3 ion−molecule chemistry as observed in ionized clusters of BBr_3. The ion distribution was observed mass spectrometrically, and observed ions were modeled with density functional theory as a means of understanding the structures of the clusters, ion−molecule reactions that can occur within them, and the development of the observed mass spectrum. A particularly novel result is the prediction that covalently bound $B_nBr_m^{\delta+}$ moieties with $n > 1$ and/or $m > 3$ are formed within the cluster ions.

Experimental Method

The locally constructed, two-chamber time-of-flight mass spectrometer used in these experiments was only slightly modified from a previous description.[8] The instrument employs a Wiley−McLaren ion acceleration scheme[9] with pulsed voltages. The acceleration pulse was typically of 5-μs duration. After acceleration, the ions passed through a coarse deflector, an einzel lens, and a pair of fine-control deflectors before entering the reflectron.

* To whom correspondence should be addressed. E-mail: hales@hendrix.edu. Tel.: 501-450-1203.

10.1021/jp065272o CCC: $37.00
Published on Web 03/03/2007

The reflectron was modified to include 90% transmission nickel screens at the entrance/exit (ground) and one-fourth of the distance back (variable potential) for clean separation of the electric fields in the two deceleration stages. Attached to the grounded entrance electrode was a shield of stiff stainless steel screen that filled the cross-sectional area of the chamber around the entrance electrode. This served to shield the field-free ion flight region from voltages on the reflectron electrodes. After energy refocusing in the reflectron, the ions exited at an angle of 5° from their initial path and impinged on a dual microchannel plate ion detector. Signal from the microchannel plates was amplified, then collected and averaged with a digital summing oscilloscope, and finally transferred to a computer for analysis.

Clusters of BBr_3 were formed by allowing a mixture of BBr_3 in helium to expand into vacuum from a variable stagnation pressure of 1−7 bar. The expansion occurred through a pulsed molecular beam valve (General Valve Series 9, 1.1-mm orifice) to which was attached a 30°-included-angle diverging conical nozzle, 1.27 cm in length. The BBr_3/He mixture was formed by bubbling He gas through liquid BBr_3 (Aldrich, >99.99%, used as received). For a stagnation pressure of 2 bar, the vapor pressure of BBr_3 at 295 K resulted in a 4% BBr_3 mixture.[10] Variation of the He pressure and the BBr_3 temperature allowed the composition of the gas mixture to be varied from 1% to 10% BBr_3.

The pulsed electron gun used in this ion source was modified slightly since its previous description.[8] The tungsten filament was enclosed in a cup-shaped repeller electrode that was capped by an extractor electrode. Following the extractor were a focusing electrode and a grounded exit orifice. The extractor and focusing electrode voltages were optimized with an eye toward both the magnitude and resolution of the ion signal, and the repeller was fixed at an appropriate negative voltage. The exit electrode was fixed at ground, and a pair of deflector plates was installed following the exit orifice. The deflector voltages were bipolar and symmetric with respect to ground potential, which allowed the electron beam to be swept across the cluster beam with minimal effect on the electron energy. The deflector setting was optimized for maximum signal, which should correspond to optimum overlap between the electron and cluster beams.

The experimental sequence began with a trigger to fire the pulsed valve. After a delay that allowed the neutral clusters to drift to the acceleration region of the mass spectrometer, the electron beam was pulsed on by dropping the extractor electrode of the electron focusing optics from the repeller voltage to an appropriate focusing voltage. The electron beam pulse typically lasted 2−3 μs. The trigger for the ion acceleration voltage pulse was simultaneous with the end of the electron beam pulse.

Experimental Results

Electron impact ionization (100 eV) mass spectra of BBr_3 clusters show five main series of cluster ions. Over several experiments varying the stagnation pressure from 2 to 4 bar and the gas mixture from 2% to 10% BBr_3, the series observed and their ranges included $B_nBr_{3n+1}^+$ ($n = 0-6$), $B_nBr_{3n}^+$ ($n = 1-7$), $B_nBr_{3n-1}^+$ ($n = 1-7$), $B_nBr_{3n-2}^+$ ($n = 1-4$), and $B_nBr_{3n-3}^+$ ($n = 1-4$). Figure 1 shows a mass spectrum acquired with 5% BBr_3 in helium at a stagnation pressure of 2 bar. Observation of five series of peaks is in sharp contrast to a similar study of BF_3 clusters where the only significant series of peaks was $B_nF_{3n-1}^+$.[8] Within any one of the five series, the cluster ions differ by an integral number of BBr_3 units. These

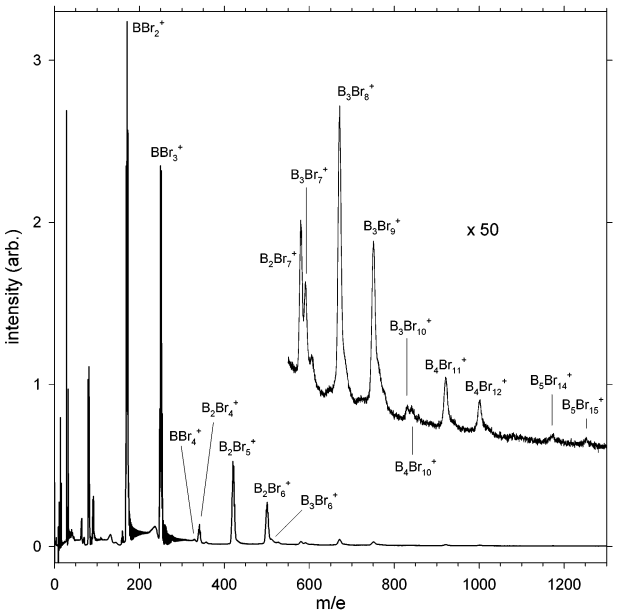

Figure 1. Sample mass spectrum obtained with 100-eV electron ionization of BBr_3 clusters.

series can be summarized as $B_nBr_{3n+m}^+$, with $m = +1$, 0, −1, −2, and −3. Cluster ions with a common m are theoretically predicted to share certain structural characteristics, as discussed below, so the various series will often be referred to by their m values.

Aside from the cluster ions, some of the lighter mass peaks observed in the mass spectra are easily identified as the normal products of electron impact on BBr_3, e.g., BBr_3^+, BBr_2^+, BBr^+, B^+, and Br^+. Each of these is present with the expected natural isotopic distribution. The relative intensities of these light ions differ from those reported for 70-eV electron ionization of BBr_3,[11] but that is not unexpected because this experiment differs in both electron energy and the use of clusters rather than isolated molecules. Small peaks corresponding to HBr^+ and Br_2^+ are also present. The presence of Br_2^+ could be due to either ion−molecule reactions within clusters or the presence of molecular bromine in the liquid BBr_3, possibly formed by decomposition of a small fraction of the BBr_3. HBr^+ indicates minor contamination of the gas inlet system with water. As is evident in Figure 1, the intensities of the $m = 0$ and $m = -1$ series are generally comparable and are much greater than those of the other three series. For larger values of n, $B_nBr_{3n}^+$ and $B_nBr_{3n-1}^+$ are dominant.

The mass spectrometer achieved unit mass resolution through BBr_3^+ ($m/z = 247-254$), and differences in Br isotopic makeup were partially resolved out to $B_2Br_6^+$. However, the lack of unit mass resolution at higher masses meant that isotopomers of any particular cluster ion were not fully resolved. Therefore, for each of the heavier cluster ions, a single peak was observed whose width was determined by the envelope of the isotopic distribution. These distributions have a width (fwhm) that is on the order of the number of bromine atoms. The result is the appearance of mass resolution that is much lower than the actual resolution of the spectrometer, which is ~350 ($m/\Delta m$) at mass 250.

Computational Method

Our computational priorities were (1) qualitative structural characteristics, i.e., what molecular fragments cling together to form the cluster ion, and (2) trends in cluster energetics. The

presence of heavy atoms such as Br meant that the inclusion of electron correlation was important for accurate energy calculations, so Hartree−Fock and other noncorrelated methods were not viable choices for this system. The geometries reported here were determined by density functional theory calculations using the B3LYP/6-31G* method as implemented in Spartan '04.[12] The requirements of this computational level combined with the flexibility of the cluster ions makes geometry optimizations of large cluster ions impractical. Therefore, we performed this analysis only for those cluster ions with 15 or fewer atoms. We also made no attempt to correct for basis set superposition error (BSSE) in these DFT calculations. Instead, we tested the effects of adding diffuse and polarization functions and use of a different correlation method by calculating energies for these optimized geometries using the B3LYP/6-311G++(2df,2p), MP2/6-31G*, and MP2/6-311G++(2df,2p) methods as implemented in Spartan '06.[12]

The geometry optimizations were performed directly from multiple asymmetric initial geometry approximations. The convergence criterion for the energy gradient was the program's default value of 4.5×10^{-4} hartree bohr^{-1}. For ions with even numbers of electrons, structures were calculated for both singlet and triplet ground states, whereas doublet and quartet states were considered for ions with odd numbers of electrons. The lower-energy result was taken to indicate the preferred multiplicity. If the optimized geometry was approximately symmetric, then the molecule was reoptimized subject to symmetry constraints. For some of the smaller ions (BBr_2^+, BBr_3^+, $B_2Br_3^+$, $B_2Br_6^+$, $B_2Br_7^+$, $B_3Br_6^+$), the symmetric structure was lowest in energy. Vibrational frequencies were calculated for all optimized structures to ensure that they corresponded to energy minima. These frequencies were also used in thermochemical calculations, as described below. All atomic charges reported here are Mulliken charges from the B3LYP/6-31G* calculations, as provided in the Spartan '04 output.

Structures were analyzed by inspection of electron density isosurfaces. A surface that encloses the volume with electron density greater than or equal to 0.002 a.u. (electrons per a_0^3) corresponds roughly to the van der Waals contact surface of a molecule. If instead the isosurface encloses only the region(s) where the electron density equals or exceeds some higher value, then the surface will enclose a smaller volume. When the surface value is set to 0.08 a.u., the area between two atoms will be enclosed within the surface if there is sufficient electron density to constitute a conventional covalent bond between those atoms. Correspondingly, a gap in the surface between two atoms can be taken to imply that there is insufficient electron density to constitute a covalent bond between those atoms. It is in this way that we distinguished between covalent bonds within molecular units and weaker interactions between such molecular units within a cluster ion.

All four methods mentioned above were used to calculate energies of the B3LYP/6-31G*-optimized structures, and these energies were used as the basis for thermochemical analyses of these cluster ions. Standard methods of statistical mechanics were used to derive translational, rotational, and vibrational contributions to enthalpy from masses, moments of inertia, and vibrational frequencies, respectively, at 298 K. The B3LYP/6-31G* vibrational frequencies were used for all thermochemistry calculations. These enthalpy contributions were added to the computed total electronic energies to find "absolute" enthalpies, H_{calc}, which were then converted to enthalpies of formation by referencing to experimental values of $\Delta_f H_{298}$ for the initial components of each cluster ion: the corresponding BBr_3 fragment ion plus the appropriate number of BBr_3 molecules. This was accomplished by adding the computational difference between $B_nBr_{3n+m}^+$ and the appropriate group of fragments to the sum of the experimental $\Delta_f H_{298}$ values for those fragments (eq 1 for $m = 0, -1, -2$, and -3; eq 2 for $m = +1$)

$$\Delta_f H(B_nBr_{3n+m}^+) = H_{calc}(B_nBr_{3n+m}^+) - [H_{calc}(BBr_{3+m}^+) + (n-1)H_{calc}(BBr_3)] + \Delta_f H[BBr_{3+m}^+(g)] + (n-1)\Delta_f H[BBr_3(g)] \quad (1)$$

$$\Delta_f H(B_nBr_{3n+1}^+) = H_{calc}(B_nBr_{3n+1}^+) - [H_{calc}(Br^+) + nH_{calc}(BBr_3)] + \Delta_f H[Br^+(g)] + n\Delta_f H[BBr_3(g)] \quad (2)$$

The required experimental values of $\Delta_f H_{298}$ for B^+, BBr^+, BBr_3^+, and Br^+ were derived by combining $\Delta_f H_{298}$ for each neutral species[13] with its ionization potential.[14] The ionization potential of BBr_2 is unavailable, so $\Delta_f H_{298}(BBr_2^+)$ was derived by combining $\Delta_f H_{298}(BBr_3)$ and $\Delta_f H_{298}(Br)$ with the appearance potential of BBr_2^+ from BBr_3.[11] The derived experimental $\Delta_f H_{298}$ values conform to the "ion convention" for treatment of the removed electron, so all the enthalpies of formation derived here are also ion convention values.[15]

Computational Results

Overview. In every case studied here, the lowest-energy structure has the lowest possible multiplicity: ions with an even number of electrons have singlet ground states, and those with an odd number have doublet ground states. Certain structural trends are readily observed. In general, cluster ions in a particular $B_nBr_{3n+m}^+$ series consist of differing numbers of BBr_3 units coordinated to a common B_nBr_{3n+m} unit, usually with $n = 2$. In almost all cases, coordination is between the Br atoms on neighboring units. Bond distances are conveniently discussed in comparison to bond lengths calculated for Br_2 and BBr_3 at the same level of theory. All Br−Br distances in these cluster ions are predicted to be longer than the bond length of neutral Br_2. B−Br distances fall into three groups. Bonds to terminal Br atoms are 2−3% shorter than a B−Br bond in neutral BBr_3. This type of bond occurs in all of the clusters studied here. Bonds from B to Br atoms that interact noncovalently with another molecular fragment within the cluster are longer than bonds in neutral BBr_3 by about 5%. In a few cases (BBr_4^+, $B_2Br_5^+$, $B_3Br_6^+$), we also see Br atoms that bridge covalently between two atoms. In this case, the B−Br bonds are about 9% longer than the B−Br bond in BBr_3.

Structures for the ions considered here are shown schematically in Chart 1. All B atoms are marked, and all other vertices and terminal positions are occupied by Br atoms. To avoid congestion in the chart, most labeled Br atoms are marked with only a lower case letter as an identifier. The long dashed lines indicate noncovalent interactions between molecular fragments. The geometries of some of the smaller ions are summarized numerically in Table 1. Coordinate tables for optimized geometries are available as Supporting Information.

Ⓦ Optimized structures for all ions discussed here are available as 3D rotatable images in pdb format.

***m* = 0**. The smallest member of the series is BBr_3^+, which retains the D_{3h} symmetry of the neutral molecule. The B−Br bonds are predicted to be 0.02 Å shorter in the ion than in the neutral molecule. The lowest-energy structure for $B_2Br_6^+$ resembles two BBr_3 units in contact through Br atoms with overall C_2 symmetry (Figure 2). Addition of atomic charges

CHART 1: Schematic Representations of Computationally Determined Structures[a]

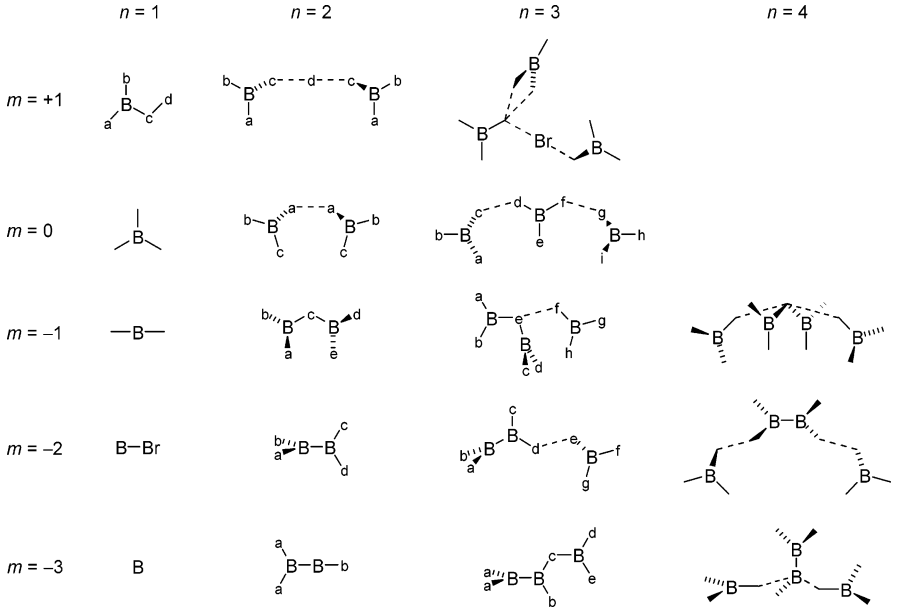

[a] B atoms are labeled; all other vertices and termini are Br atom positions.

shows that the charge is shared equally across both BBr_3 units, a condition that is expected here because of symmetry. The distance between the linking Br atoms is 3.277 Å, markedly longer than that calculated for neutral Br_2. The structure predicted for $B_3Br_9^+$ is an extension of the $B_2Br_6^+$ structure, with two Br···Br interactions. Compared to $B_2Br_6^+$, the Br···Br distances are longer (4.021 and 4.033 Å vs 3.277 Å), and the B−Br···Br angles are larger (123−126° vs 118.7°). The charge is spread among all three BBr_3 units with slightly less on the central moiety (+0.294) as compared to the outer units (+0.353 each).

***m* = −1.** The smallest member of this series is BBr_2^+, which our calculations predict to be linear with $D_{\infty h}$ symmetry, as expected for a 16-valence-electron AB_2 molecule.[16] The second member of this series is $B_2Br_5^+$, whose structure does not contain an identifiable BBr_2^+ fragment, but instead involves a bridging Br atom in a structure with approximate C_2 symmetry (Figure 3). All larger members of the series for which structures were calculated include the B_2Br_5 fragment, although it is significantly twisted in the case of $B_3Br_8^+$. $B_4Br_{11}^+$ has two BBr_3 units coordinated to the B_2Br_5 moiety in a manner that results in approximate C_2 symmetry. $B_3Br_8^+$ and $B_4Br_{11}^+$ stand out in that they show the greatest concentrations of charge on a single fragment of any of the cluster ions studied here: addition of atomic charges places the charge on the B_2Br_5 fragment at +0.975 and +0.983 in $B_3Br_8^+$ and $B_4Br_{11}^+$, respectively, so the coordinating BBr_3 molecules are essentially neutral in each of these cases. Another feature common to these two cluster ions is that the primary intermolecular interaction within each cluster is between BBr_3 bromine atoms and the central Br of the B_2Br_5 fragment. For $B_3Br_8^+$, this is also the closest contact point between the two molecules. In $B_4Br_{11}^+$, the BBr_3 bromine atom is slightly closer to a B atom in B_2Br_5 (3.998 Å, 4.094 Å) than to the central Br atom (4.110 Å, 4.112 Å), although the electron density along the Br−Br line is greater at its minimum by 10% than that along the B−Br line.

***m* = −2.** This series is one of only two, along with $B_nBr_{3n-3}^+$, in which adjacent B atoms are predicted. The smallest ion in this series is BBr^+. Previous theoretical predictions of the BBr^+ bond length have varied, including such values as 1.743 Å [CCSD(T)/CBS with scalar relativity and core−valence correlation],[17] 1.755 Å (CASSCF+CI with averaged atomic natural orbital basis sets),[18] and 1.766 Å (B3LYP/cc-pVDZ).[19] There is no obvious trend in these values with level of theory, but our computational bond length of 1.761 Å falls in their midst. $B_2Br_4^+$, observed previously in mass spectrometric analysis of a B_2Br_4 sample,[20] has approximate D_{2d} symmetry. The structure with exact D_{2d} symmetry is higher in energy, but by only 3.1×10^{-5} hartree ≈ 0.08 kJ mol^{-1}. $B_2Br_4^+$ is a single covalently bound entity, as seen above for $B_2Br_5^+$. Larger members of this series have BBr_3 molecules coordinated through Br atoms to Br atoms of a B_2Br_4 unit. $B_4Br_{10}^+$, which has approximate C_2 symmetry (Figure 4), differs from $B_3Br_7^+$ only by the presence of a second BBr_3 molecule. The bond lengths and bond angles of the $B_3Br_7^+$ fragment within $B_4Br_{10}^+$ differ from the equivalent entities in the optimized structure of $B_3Br_7^+$ by no more than 0.025 Å and 2°, except for "intermolecular" quantities: the Br···Br distance (0.19 Å), a B−Br···Br angle (6.3°), and the B−Br···Br−B dihedral angle (7°).

***m* = −3.** The $n = 1$ member of the $B_nBr_{3n-3}^+$ series is the atomic ion B^+, so our discussion begins with $B_2Br_3^+$. This ion finds its minimum energy in a planar C_{2v} structure. This structure is homologous to BBr_2^+ in that it can be formed from the latter by replacing −Br with $-BBr_2$. $B_2Br_3^+$ was observed in the same experiment as $B_2Br_4^+$; among all ions reported here with more than four atoms, they are the only two ions to have been observed previously.[20] $B_3Br_6^+$ (C_s symmetry) is a single covalently bound unit according to the electron density criteria described above. BBr_3 and B_2Br_3 substructures are apparent, but it is best described as a homologue of $B_2Br_5^+$ in which one of the terminal Br atoms has been replaced with $-BBr_2$. Electron density isosurfaces indicate that $B_4Br_9^+$ can be represented as a cluster of three separate units: two BBr_3 units are coordinated through Br atoms to the unsaturated B atom of a bent B_2Br_3 unit ($Br_2B-B-Br$ angle = 135°). This is the only case studied here in which Br → B coordination between fragments is computationally predicted.

***m* = +1.** BBr_4^+ is a single, covalently bound, planar unit in which an "extra" Br is attached to a Br atom of BBr_3. In $B_2Br_7^+$, a second BBr_3 is coordinated to the extra Br atom in

TABLE 1: Computational Geometries of Selected Species (B3LYP/6-31G*)[a]

species	bond length (Å)		bond angle (deg)		dihedral angle (deg)	
			neutrals			
Br_2	Br−Br	2.324				
BBr_3	B−Br	1.919	Br−B−Br	120.00		
			$m = 0$			
BBr_3^+	B−Br	1.899	Br−B−Br	120.00		
$B_2Br_6^+$	B−a	1.962	a−B−b	113.12	a−a−B−b	−173.46
	B−b	1.897	a−B−c	121.52	a−a−B−c	6.42
	B−c	1.882	b−B−c	125.36	B−a−a−B	−70.33
	a−a	3.277	B−a−a	118.71		
			$m = -1$			
BBr_2^+	B−Br	1.771	Br−B−Br	180.00		
$B_2Br_5^+$	B−a	1.862	a−B−b	129.04	a−B−c−B	−15.77
	B−b	1.867	a−B−c	120.40	b−B−c−B	167.88
	(b−)B−c	2.083	b−B−c	110.43	d−B−c−B	154.47
	(d−)B−c	2.091	B−c−B	116.34	e−B−c−B	−29.76
	B−d	1.866	c−B−d	110.95		
	B−e	1.862	c−B−e	119.55		
			d−B−e	129.33		
			$m = -2$			
BBr^+	B−Br	1.761				
$B_2Br_4^+$	B−B	1.882	a−B−b	134.04	a−B−B−c	−89.87
	B−a	1.864	c−B−d	133.97	a−B−B−d	90.10
	B−b	1.864	B−B−a	113.04	b−B−B−c	90.14
	B−c	1.865	B−B−b	112.92	b−B−B−d	−89.89
	B−d	1.865	B−B−c	113.13		
			B−B−d	112.90		
			$m = -3$			
$B_2Br_3^+$	B−B	1.665	a−B−B	180.00		
	B−a	1.768	B−B−b	116.29		
	B−b	1.886				
$B_3Br_6^+$	B−B	1.685	a−B−B	117.87	a−B−B−b	89.53
	B−a	1.902	B−B−b	128.78	a−B−B−c	90.47
	B−b	1.859	B−B−c	109.37	B−B−c−B	180.00
	(b−)B−c	2.092	B−c−B	120.42	b−B−c−B	0.00
	(d−)B−c	2.086	c−B−d	110.05	B−c−B−d	180.00
	B−d	1.868	c−B−e	120.79	B−c−B−e	0.00
	B−e	1.861				
			$m = +1$			
BBr_4^+	B−a	1.867	a−B−b	133.86	a−B−c−d	180.00
	B−b	1.846	a−B−c	105.91	b−B−c−d	0.00
	B−c	2.089	B−c−d	109.86		
	c−d	2.334				
$B_2Br_7^+$	B−a	1.878	a−B−b	126.40	a−B−c−d	−4.68
	B−b	1.882	a−B−c	120.46	b−B−c−d	175.38
	B−c	2.010	B−c−d	108.29	B−c−d−c	142.43
	c−d	2.614	c−d−c	178.38		

[a] Lower case letters refer to Br atom labels in Chart 1.

BBr_4^+. In this C_2-symmetric ion, the Br···Br···Br angle through the central Br atom is very nearly linear at 178.4°. The Br−Br distances are greater in $B_2Br_7^+$ (2.61 Å) than in BBr_4^+ (2.33 Å), and it is best described as two BBr_3 units coordinated to a central Br atom. The charge is distributed evenly over the two BBr_3 units, whereas the central Br atom is nearly neutral at +0.060. $B_3Br_{10}^+$ includes the $B_2Br_7^+$ structure with a third BBr_3 molecule loosely attached to a bridging Br atom in one of its BBr_3 molecules. The geometry of the B_2Br_7 unit is nearly unchanged by the addition of the third BBr_3 molecule, as bond lengths and bond angles are found to differ by less than 0.002 Å and 1°, respectively. The only significant change in the geometry of the B_2Br_7 unit is the B−Br(−Br)−Br−B dihedral angle, which is greater in $B_3Br_{10}^+$ (127.6°) than in $B_2Br_7^+$ (75.5°). The charge on the third BBr_3 molecule in this cluster ion is only +0.013, much less than the charges of +0.452 and +0.476 on the two BBr_3 moieties in the B_2Br_7 unit.

Thermochemistry. Enthalpies of formation for the ions addressed here, calculated as described above, are listed in Table 2. These $\Delta_f H_{298}$ values were used to determine reaction enthalpies for two classes of reactions. Elimination of BBr_3 molecules from cluster ions is an important process in the development of the observed mass distribution, and predicted enthalpy changes for that process are listed in Table 3. Reactions forming the core ion of each series as an adduct between BBr_3 and an appropriate BBr_3 fragment ion are also of interest. Enthalpies of these reactions are easily found from ΔH(BBr_3 elimination), as each addition reaction is simply the reverse of one of the BBr_3 elimination reactions.

The uncertainties listed in Table 2 are wholly derived from experimental uncertainties in ionization potentials ($m = 0, -2$) and an appearance potential ($m = -1$). No uncertainties are

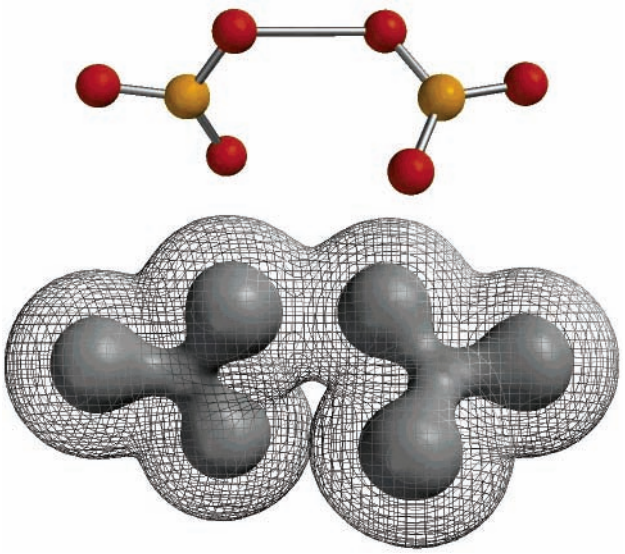

Figure 2. Optimized structure and electron density isosurfaces for $B_2Br_6^+$, all at the same scale but offset for clarity. The light colored balls represent B atoms, and the darker balls represent Br atoms. The mesh surface represents an electron density of 0.002 a.u. and corresponds approximately to the van der Waals contact surface. The solid surface represents an electron density of 0.08 a.u. and encloses regions of sufficient electron density to be considered covalent bonds.

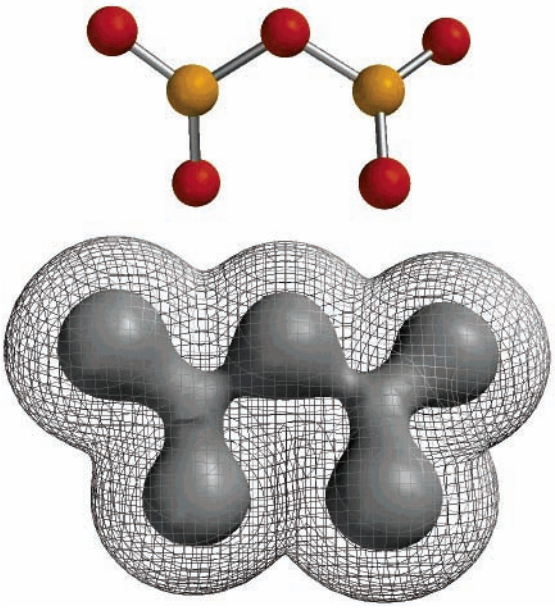

Figure 3. Optimized structure and electron density isosurfaces for $B_2Br_5^+$. The structure and isosurfaces are as in Figure 2.

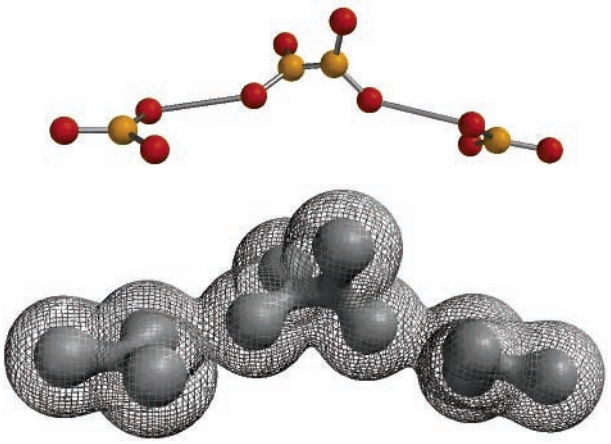

Figure 4. Optimized structure and electron density isosurfaces for $B_4Br_{10}^+$. The structure and isosurfaces are as in Figure 2.

TABLE 2: Computational Enthalpies of Formation, kJ mol^{-1}

	B3LYP/6-31G*	B3LYP/ 6-311++G (2df,2p)	MP2/ 6-31G*	MP2/ 6-311++G (2df,2p)
		neutral		
BBr_3(g)	−204.18[a]	−204.18[a]	−204.18[a]	−204.18[a]
		$m = 0$		
BBr_3^+	809.9 ± 2[b]	809.9 ± 2[b]	809.9 ± 2[b]	809.9 ± 2[b]
$B_2Br_6^+$	548.8 ± 2	593.6 ± 2	557.0 ± 2	544.2 ± 2
$B_3Br_9^+$	326.7 ± 2	392.6 ± 2	420.6 ± 2	388.4 ± 2
		$m = -1$		
BBr_2^+	716.0 ± 20[b]	716.0 ± 20[b]	716.0 ± 20[b]	716.0 ± 20[b]
$B_2Br_5^+$	456.4 ± 20	473.7 ± 20	443.4 ± 20	425.2 ± 20
$B_3Br_8^+$	256.5 ± 20	289.1 ± 20	224.2 ± 20	196.0 ± 20
$B_4Br_{11}^+$	62.7 ± 20	110.7 ± 20	18.6 ± 20	N/A[c]
		$m = -2$		
BBr^+	1267.0 ± 20[b]	1267.0 ± 20[b]	1267.0 ± 20[b]	1267.0 ± 20[b]
$B_2Br_4^+$	780.2 ± 20	794.8 ± 20	799.4 ± 20	783.0 ± 20
$B_3Br_7^+$	556.7 ± 20	591.7 ± 20	604.2 ± 20	583.4 ± 20
$B_4Br_{10}^+$	345.7 ± 20	400.1 ± 20	401.5 ± 20	376.4 ± 20
		$m = -3$		
B^+	1360.6[b]	1360.6[b]	1360.6[b]	1360.6[b]
$B_2Br_3^+$	723.7	728.2	764.4	746.1
$B_3Br_6^+$	464.6	485.0	483.3	445.0
$B_4Br_9^+$	269.0	305.4	256.7	198.0
		$m = +1$		
Br^+	1251.7[b]	1251.7[b]	1251.7[b]	1251.7[b]
BBr_4^+	745.7	744.0	803.3	747.9
$B_2Br_7^+$	475.8	495.8	546.0	473.7
$B_3Br_{10}^+$	278.2	312.3	333.8	253.0

[a] Experimental value from ref 13. [b] Calculated from experimental values as described in text. [c] Our hardware was insufficient to complete the calculation for $B_4Br_{11}^+$.

listed for some species because either the quantities used to determine those values are known with significantly greater precision [IP(B), ±0.002 kJ mol^{-1}][14] or no uncertainty is provided in the reference {Δ_fH[BBr_3(g)], Δ_fH[B(g)], Δ_fH[Br(g)], IP(Br)}.[13,14] No uncertainties are listed for reaction enthalpies because the uncertainties in the Δ_fH_{298} values within a series all arise from the same source, and so have the same magnitude and direction, cancelling out in the calculation of differences. The enthalpies of reaction are thus reflective of only the computational results with no contributions from the experimental values used to find Δ_fH_{298}.

For reasons discussed below, all thermochemical values cited in the Discussion are from the MP2/6-311++G(2df,2p) model.

TABLE 3: Computational Enthalpies of BBr_3 Elimination, kJ mol^{-1}

	B3LYP/6-31G*	B3LYP/ 6-311++G (2df,2p)	MP2/ 6-31G*	MP2/ 6-311++G (2df,2p)
		$m = 0$		
$B_2Br_6^+$	56.9	12.1	48.7	61.5
$B_3Br_9^+$	17.9	−3.1	−67.8	−48.4
		$m = -1$		
$B_2Br_5^+$	55.4	38.1	68.4	86.6
$B_3Br_8^+$	−4.3	−19.6	15.1	25.0
$B_4Br_{11}^+$	−10.4	−25.7	1.4	N/A
		$m = -2$		
$B_2Br_4^+$	282.6	268.0	263.4	279.9
$B_3Br_7^+$	19.3	−1.1	−9.0	−4.6
$B_4Br_{10}^+$	6.8	−12.5	−1.4	2.8
		$m = -3$		
$B_2Br_3^+$	432.7	428.2	392.0	410.3
$B_3Br_6^+$	54.9	39.0	76.9	96.9
$B_4Br_9^+$	−8.6	−24.6	22.4	42.8
		$m = +1$		
BBr_4^+	301.8	303.6	244.2	299.6
$B_2Br_7^+$	65.7	43.9	53.1	70.1
$B_3Br_{10}^+$	−6.6	−20.6	8.0	16.5

Discussion

Structures and Reactions. The formulas of the five series of ions observed correspond exactly to addition of BBr_3 molecules to each of the five ions that can be formed in electron ionization of BBr_3. The structures expected from this description, assuming no additional bond formation or breakage, would look like BBr_3 molecules clustered around BBr_3^+, BBr_2^+, BBr^+, B^+, and Br^+ for $m = 0$, −1, −2, −3, and +1, respectively. The computational results predict that the cluster ion structures do resemble BBr_3 molecules coordinated to a central ion, although the central ion is not always an electron ionization product of BBr_3. These deviations of the calculated structures from the simplest possibilities indicate that ion−molecule reactions have taken place within those clusters. In most cases, the positive charge is not localized on one fragment in the cluster ion, but is shared throughout the cluster. This indicates that the clusters are not held together solely by intermolecular electrostatic forces, so the structures cannot be predicted and the computationally determined structures cannot be justified solely on the basis of electrostatic interactions between an ion and the BBr_3 molecules that surround it.

Examination of the predicted cluster ion structures reveals a trend in intermolecular contacts within the clusters. In $B_4Br_9^+$, from the most bromine-deficient series, there are two BBr_3 molecules coordinated to one of the B atoms in the central B_2Br_3 moiety, and $B_4Br_{11}^+$ has one BBr_3 molecule coordinated in a somewhat ambiguous fashion to each face of the central B_2Br_5 moiety (see below). Aside from these exceptions, all intermolecular contacts within the clusters are Br to Br. This differs from the structures calculated for $B_nF_{3n-1}^+$, where F → B coordination is dominant.[8] The F → B coordination observed previously was explained as arising from electrostatic interactions between closed-shell fragments within the clusters. The high electronegativity of fluorine results in a greater degree of charge separation along B−F bonds in $B_nF_{3n-1}^+$ than would be expected for bonds in $B_nBr_m^+$. Therefore, the strength of the intermolecular electrostatic forces should be lower with bromine than with fluorine, and apparently these forces are not sufficient to control the geometry in the $B_nBr_m^+$ case.

Electron ionization of a molecule forms an excited ion that then can break into fragments. When this happens to a molecule

within a cluster, the fragment ion also interacts with nearby neutral molecules. Any energy released in a reaction can be carried away by evaporation of molecules from the cluster, so the formation of stable adducts is possible. The resulting observed cluster ion distribution is the result of both reactions within and evaporation of neutral molecules from the clusters. The computational results above imply the formation of adducts in most cases, although the reactions do not appear to continue indefinitely. Larger members of the $m < 0$ series are best represented as adduct ions that are solvated by some number of BBr_3 molecules, whereas larger members of the $m = 0$ and $+1$ series consist of BBr_3 molecules solvating ions produced in electron ionization of BBr_3. The formation of each series is discussed in turn below.

***m* = 0.** This series is the only one observed here in which all of the ions can be formed without the formation or breakage of covalent bonds. BBr_3^+ ions simply are solvated by surrounding neutral BBr_3 molecules. In these clusters, excess energy from the ionization process is dissipated by cluster evaporation rather than ion fragmentation. As noted above, the B−Br distance in BBr_3 is predicted to decrease very slightly upon ionization to BBr_3^+. The HOMO of neutral BBr_3 consists of one p orbital from each Br atom, perpendicular to the B−Br bond and in the molecular plane. The three Br orbitals are arranged such that all Br−Br interactions are between lobes of opposite phase (C_{3h} symmetry). This molecular orbital is B−Br nonbonding, so removal of electron density from it should have a small effect if any on the B−Br bonds. The small decrease in bond length can be rationalized in that removal of electron density from this molecular orbital should result in less repulsion between the Br atoms, allowing them to move in closer to the central B atom.

Cluster ions in this series consist of groups of BBr_3 units interacting through Br···Br contacts. The Br−Br distances are all significantly greater than predicted for neutral Br_2, which can be taken to indicate an interaction much weaker than the covalent bond in the Br_2 molecule. This notion also is supported by the 0.08 a.u. electron density isosurface shown as the solid surface in Figure 2. As cluster size grows, an approach toward the behavior of bulk neutral molecules would be expected. The greater Br−Br distances and shorter bonds between B and bridging Br atoms in $B_3Br_9^+$ as compared to $B_2Br_6^+$, both of which indicate a weaker intermolecular interaction in the larger cluster, are in line with this idea.

***m* = −1.** The members of this series are structurally similar to those in the analogous series formed by ionization of BF_3 clusters, but generally less symmetric.[8] This series begins formally with BBr_2^+, but all heavier ions in the series include the $B_2Br_5^+$ fragment. $B_2Br_5^+$ is the adduct between BBr_2^+ and a neutral BBr_3 molecule, the formation of which is predicted to be exothermic by 86.6 kJ mol^{-1}. A pair of orbitals that can overlap favorably in the mutual approach of these two species are the LUMO of BBr_2^+ and the HOMO of BBr_3 (Figure 5a). The overlap is π-type between the lobes on a Br atom of BBr_3 and the B atom of BBr_2^+. Donation of electron density into the BBr_2^+ LUMO, which is B−Br antibonding, is consistent with the increase in the B−Br bond length from BBr_2^+ to $B_2Br_5^+$.

The prediction that the B_2Br_5 fragments in $B_3Br_8^+$ and $B_4Br_{11}^+$ carry nearly complete $+1$ charges implies that minimal electron sharing takes place between fragments within these clusters. There is some ambiguity in the interaction of the BBr_3 molecules in $B_4Br_{11}^+$ with the central B_2Br_5 fragment, as described above. The fact that the electron density along the B−Br line (shorter distance) dips lower than that along the Br−Br line (longer distance) can be understood by comparing the interatomic distances in question to typical B−Br and Br−Br bond lengths. The average of the two B−Br distances in question in $B_4Br_{11}^+$ is 2.11 times the B−Br distance in BBr_3, but the corresponding Br−Br distances average to only 1.77 times the Br_2 bond length. This is the reasoning behind the structure shown in Chart 1, although the interaction between Br atoms appears to be only slightly stronger than that between B and Br atoms.

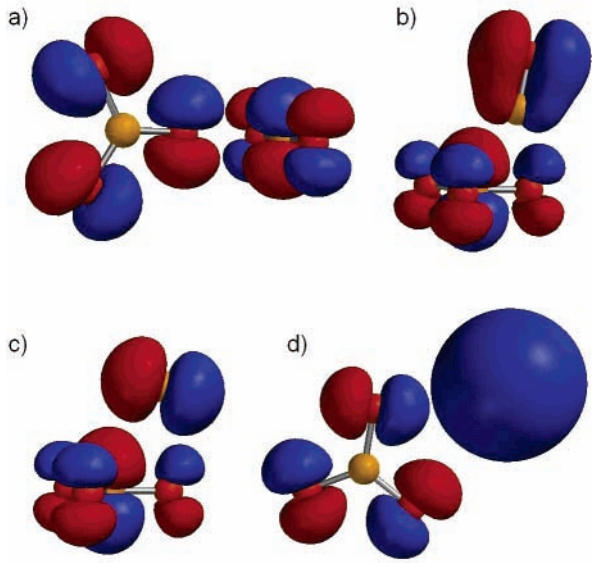

Figure 5. Possible approaches leading to adduct formation within cluster ions: (a) BBr_2^+ (LUMO) + BBr_3 (HOMO) → $B_2Br_5^+$, (b) BBr^+ (highest filled MO) + BBr_3 (LUMO) → $B_2Br_4^+$, (c) excited B^+ (HOMO) + BBr_3 (LUMO) → $B_2Br_3^+$, (d) Br^+ (LUMO) + BBr_3 (HOMO) → BBr_4^+.

BF_2^+ is the dominant ion formed in electron ionization of BF_3,[21] which is why $B_nF_{3n-1}^+$ was the dominant series observed in electron ionization of $(BF_3)_n$.[8] Likewise, BBr_2^+ is the dominant ion formed in electron ionization of BBr_3.[11] In this context, the prominence of the $m = -1$ series is no surprise.

***m* = −2.** The B_2Br_4 structure is homologous to BBr_3 in that it can be formed by substituting $-BBr_2$ for $-Br$ in BBr_3. It is likely the product of adduct formation between BBr^+ and BBr_3. The predicted structure, with neighboring B atoms, implies that there is an insertion of the B end of BBr^+ into a B−Br bond of BBr_3. We suggest that this insertion begins with BBr^+ approaching BBr_3 as shown in Figure 5b. The highest fully occupied orbital of BBr^+ (there is a singly occupied orbital at slightly higher energy) can donate electron density to the LUMO of BBr_3, which will weaken the B−Br bonds in BBr_3 and allow the BBr^+ to insert its B atom into one of those bonds. This reaction is predicted to be significantly exothermic with $\Delta H = -279.9$ kJ mol^{-1}.

Larger ions in this series all include the B_2Br_4 fragment. The HOMO of $B_2Br_4^+$ (singly occupied in the ion) is σ-bonding between B atoms and includes favorable interaction between the pair of Br atoms at either end of the molecule. Therefore, additional electron density in this molecular orbital should reduce the B−B distance and the Br−B−Br angles. In the geometry predicted for $B_3Br_7^+$, the HOMO of BBr_3 overlaps effectively with this MO, donating some charge density into it as $B_3Br_7^+$ is formed and reducing the charge on B_2Br_4 from $+1$ to $+0.667$. The same process is repeated at the other end of the molecule to form $B_4Br_{10}^+$, which further reduces the charge on the B_2Br_4 fragment to $+0.486$. The B−B distances

TABLE 4: Geometry of B_2Br_4 Moiety within $m = -2$ Cluster Ions

ion	B−B distance (Å)	Br−B−Br angle (deg)
$B_2Br_4^+$	1.822	133.97, 134.04
$B_3Br_7^+$	1.746	127.55, 127.66
$B_4Br_{10}^+$	1.723	125.45, 125.62

and Br−B−Br angles change exactly as expected for electron density donation into the B_2Br_4 HOMO (Table 4). The two Br−B−Br angles in each case differ by less than 0.2°, even for the asymmetrically coordinated B_2Br_4 unit in $B_3Br_7^+$.

***m* = −3.** The formula for $B_2Br_3^+$ corresponds to adduct formation between BBr_3 and B^+. The LUMO of BBr_3 is π-antibonding between B and each Br. Electron ionization at 100 eV is an energetic technique, and it is quite likely that some fraction of the B^+ ions are formed in the two lowest excited terms, i.e., ^3P at 4.63 eV and ^1P at 9.10 eV, each with a nominal electron configuration of $[He]2s^12p^1$.[22] As the occupied 2p orbital of such an excited B^+ overlaps with the BBr_3 LUMO (Figure 5c), the donation of electron density into the LUMO will weaken the B−Br bond, easing insertion of B^+ to form $B_2Br_3^+$ with the computationally predicted structure.

Computational thermochemistry predicts formation of $B_2Br_3^+$ from BBr_3 and B^+ to be highly exothermic with $\Delta H = -410.3$ kJ mol^{-1}, assuming ground-state reactants. Starting with the excited states specified above, the reaction would release 857 or 1288 kJ mol^{-1}, respectively, if ground-state products were formed. This large amount of energy must be dissipated by some mechanism in order for the adduct to survive. The amount of energy removed per evaporated molecule is much smaller than these amounts, so complete evaporation of the cluster and/or fragmentation of the newly formed $B_2Br_3^+$ ion might be common outcomes. This would explain the overall low intensity of the series despite the favorable thermochemistry for $B_2Br_3^+$ formation.

$B_3Br_6^+$ is a single covalently bound unit, which does not comply with the pattern of BBr_3 molecules coordinating to the $n = 2$ ion as seen in the $m = -1$ and -2 series. The clue to the cause of this behavior lies in the structure's similarity to $B_2Br_5^+$. Both of these species can be viewed as coming from a BBr_3 molecule adding to the unsaturated B atom in an ion, either BBr_2^+ or $B_2Br_3^+$. In $B_4Br_9^+$, two BBr_3 molecules are coordinated via Br atoms to the unsaturated B atom of a B_2Br_3 unit. The intermolecular B−Br distances differ significantly at 2.204 and 3.107 Å. The shorter of these two is not far off the typical distance of ∼2.1 Å between B and a covalently bridging Br. Inspection of the $B_4Br_9^+$ electron density isosurface shows that this particular connection is almost enclosed within the surface: the electron density is only slightly below the arbitrary cutoff for what is considered a covalent bond. It is almost equally valid to consider $B_4Br_9^+$ to be one BBr_3 unit coordinated to $B_3Br_6^+$ as it is to treat it as two BBr_3 molecules coordinated to $B_2Br_3^+$.

***m* = +1.** This series should arise from formation of Br^+ within a BBr_3 cluster. Our computations predict that the reaction $Br^+ + BBr_3 \rightarrow BBr_4^+$ is exothermic by 299.6 kJ mol^{-1}. The ground electron configuration of Br^+ includes two unpaired electrons in 4p orbitals, so interaction between the singly occupied Br^+ HOMO and the BBr_3 LUMO, similar to that shown in Figure 5c, could lead to insertion of the Br atom to yield BBr_4^+. Alternatively, it also is possible that the initial interaction between Br^+ and BBr_3 is σ overlap between one lobe of the BBr_3 HOMO and the Br^+ LUMO, which is its 5s orbital. This would lead naturally to a nonlinear B−Br−Br angle (Figure 5d). Whatever the mechanism for its formation, the Br−Br bond in BBr_4^+ is only 0.01 Å longer than that in Br_2, implying a rough equivalence between these two Br−Br linkages.

The Br−Br interactions in $B_2Br_7^+$ are quite different. The substantial increase in length compared to BBr_4^+ is in accord with the electron density isosurface that shows a gap in each region between Br atoms. The implication is that the Br^+ is unable to make two bonds to BBr_3 that are as strong as the lone Br−Br bond in BBr_4^+. This conclusion is also supported thermochemically, as removal of BBr_3 from $B_2Br_7^+$ is predicted to be only 70.1 kJ mol^{-1} endothermic, as compared to 299.6 kJ mol^{-1} for BBr_4^+. $B_2Br_7^+$ thus appears to be a Br^+ ion that is solvated by two BBr_3 molecules.

To extend this analysis to $B_3Br_{10}^+$, consider it to be a $B_2Br_7^+$ unit with an added BBr_3 molecule. This third BBr_3 moiety does not interact directly with the central Br atom, but instead interacts with one of the BBr_3 molecules in the $B_2Br_7^+$ unit. The third BBr_3 is essentially neutral, with a charge of only +0.005. The presence of the third BBr_3 leaves the geometry of the $B_2Br_7^+$ unit almost unchanged, and the enthalpy cost for its removal from $B_3Br_{10}^+$ is predicted to be significantly less than that required for BBr_3 elimination from $B_2Br_7^+$. This interaction is so much weaker than those in $B_2Br_7^+$ that it might be taken to be the beginning of a second solvation shell for the Br^+ ion. In this picture, the first solvation shell for Br^+ is complete with two BBr_3 molecules. If additional BBr_3 molecules are attached to this system with equally weak interactions, then the low intensity of those cluster ions in the mass spectrum is quite reasonable.

Thermochemical Trends. Within any single series of ions, the calculated values for enthalpy of formation decrease with increasing cluster size. In the limit of very large cluster size, a cluster ion becomes essentially a droplet of liquid BBr_3 with a small perturbation due to the presence of a single solvated ion. Therefore, as n becomes very large, we would expect Δ_fH_{298} to approach the value of $\Delta_fH_{298}[BBr_3(l)] = -238.49$ kJ mol^{-1}.[23] Although none of the ions treated here has $\Delta_fH_{298} < 0$, all five series show trends in this direction with increasing n, regardless of computational method.

All four reactions that form adduct ions from BBr_3 fragment ions and BBr_3 molecules are predicted to be exothermic, as is the reaction forming the $B_2Br_6^+$ complex. The reactions with the most negative enthalpies are those forming BBr_4^+, $B_2Br_3^+$, and $B_2Br_4^+$, and the exothermicity of the reaction forming $B_2Br_6^+$ is much lower. The obvious difference among these cases is that the first three are cluster ions in which all atoms are joined covalently in a single molecular unit whereas $B_2Br_6^+$ consists of a pair of BBr_3 units held together by a weaker interaction. The surprise, then, is that the enthalpy of the reaction forming $B_2Br_5^+$ is much closer to that for $B_2Br_6^+$ than it is to those for BBr_4^+, $B_2Br_3^+$, and $B_2Br_4^+$, even though the seven atoms in $B_2Br_5^+$ comprise a single covalently bound molecular unit. This might be due in large part to the relatively high stability of the BBr_2^+ ion, which is a reactant in the formation of $B_2Br_5^+$.

Elimination of BBr_3 is most endothermic for small clusters and becomes gradually less endothermic as cluster size increases. As any cluster ion breaks apart, the attractive interaction between the charge on one fragment and the induced dipole (or permanent dipole) on the other fragment resists the separation. The charge is more localized on smaller cluster ions, so the barrier to separation presented by this attractive force is greater for smaller cluster ions. This charge−induced dipole force is

stronger and operates over longer distances than the induced dipole−induced dipole interactions present in the bulk liquid.[24] The enthalpy of BBr_3 elimination from these small cluster ions should therefore be no less than the bulk enthalpy of vaporization, which is 34.4 ± 0.1 kJ mol^{-1}.[23] With all four computational methods used here, each ion that is predicted to be a single covalently bound unit has ΔH(BBr_3 elimination) > $\Delta_{vap}H$(BBr_3). Among the clusters that include molecular fragments held together by noncovalent forces, the number meeting this standard varies by computational method. In some clusters, we even see negative values.

This situation provides criteria by which we can compare the different computational methods used here. Values for ΔH(BBr_3 elimination) that are positive but less than $\Delta_{vap}H$[BBr_3(l)] are clearly too low. Negative values, which would indicate instability toward dissociation of clusters that are experimentally observed, are even further off the mark. The MP2/6-311++G(2df,2p) method fares best by these criteria, as it has both the fewest values of ΔH(BBr_3 elimination) < $\Delta_{vap}H$[BBr_3(l)] and the fewest negative values for ΔH(BBr_3 elimination). For this reason, we have used thermochemical values derived by this method throughout this Discussion. Interestingly, the method that fares worst for nearly all clusters is B3LYP/6-311++G(2df,2p). The addition of diffuse functions might be expected to yield improved thermochemical results in clusters that include noncovalent interactions, and expansion of the basis set from 6-31G* does result in more positive (or less negative) dissociation enthalpies for all of these cluster ions under MP2. However, the results with the expanded basis set are actually less reasonable under B3LYP.

For MP2/6-311++G(2df,2p), apparently the best of these four methods, only $B_2Br_6^+$, $B_2Br_7^+$, and $B_4Br_9^+$ among clusters with noncovalent interactions have ΔH(BBr_3 elimination) > $\Delta_{vap}H$(BBr_3), and $B_3Br_7^+$, $B_3Br_8^+$, $B_3Br_9^+$, $B_3Br_{10}^+$, and $B_4Br_{10}^+$ have values that are too low. One possible explanation for low ΔH(BBr_3 elimination) values would be that we did not locate global minimum-energy structures for those cluster ions, despite using several different initial geometries for each cluster, including structures with networked B atoms, chains of B atoms, and structures with bridging Br atoms. However, with the single exception of $m = -3$ with MP2/6-311++G(2df,2p), low enthalpies of BBr_3 elimination appear to be a problem across all series and with all methods. Therefore, it seems likely that these computational treatments systematically underestimate the strength of intermolecular interactions within these cluster ions, even with a basis set including diffuse functions. It also is notable that, by the criteria used above, MP2 yields improved results over B3LYP for singlet species ($m = -3, -1, +1$), but the results for doublet species ($m = -2, 0$) are less reasonable than those from B3LYP/6-31G*. This apparent discrimination between singlet and doublet species also points to shortcomings in the computational treatments used here, at least for this chemical system. Overall, it seems clear that the enthalpies of BBr_3 elimination in Table 3 should be viewed with caution, particularly for larger cluster ions. However, even though some of the values themselves are clearly too low to be realistic, the trend of these values within a series is reasonable.

Structural Caveats. When a computational geometry optimization is successful, the end result is a minimum-energy static structure. The process by which the ions are made, however, is quite energetic and results in cluster ions with some amount of internal energy. Evaporation of neutral molecules provides a means of disposal for much of that energy, but evaporation will end when the internal energy of the cluster ion is less than the amount of energy required for the next evaporation step. The enthalpy of BBr_3 elimination from a cluster is therefore an upper limit for the amount of internal energy left in that cluster if evaporation is no longer possible. As discussed in the previous section, the enthalpy of BBr_3 elimination for any given step should be no less than $\Delta_{vap}H$(BBr_3) = 34.4 kJ mol^{-1}, and higher values are predicted for the smallest cluster ions. Therefore, the clusters can have significant internal energies when the evaporation process is complete. This will result in clusters that explore a variety of conformations. However, once the internal energy is low enough for evaporation to cease, it also will be low enough that covalent bonds should remain intact. The theoretical predictions about cluster composition in terms of molecular fragments held together in a cluster by noncovalent interactions should hold, although internal energy might cause the arrangement of the fragments relative to each other to vary from the computationally predicted structures.

Conclusions

We observed a series of cluster ions corresponding to each of the five ions that can be formed by electron ionization of BBr_3 and found the relative intensities of the series to be roughly parallel to the observed relative intensities of the BBr_3 fragment ions in the mass spectrum. These facts imply that each cluster ion results from ionization and fragmentation of a single BBr_3 molecule within the cluster. Our computational studies predict that exothermic reactions take place within many of the clusters to form covalently bound species that are larger than BBr_3. In each case, the formation of new covalent bonds can continue until there are no remaining unsaturated B atoms. BBr_2^+ and BBr^+ each require one BBr_3 molecule to complete the process: the B in BBr_2^+ attaches to a Br of BBr_3 and BBr^+ inserts its B atom into a B−Br bond so that their B atoms all have three bonds. B^+, however, requires two BBr_3 molecules: B^+ inserts into a B−Br bond to form $B_2Br_3^+$, and the divalent B atom in that species can then bond to a Br atom of a second BBr_3 to form $B_3Br_6^+$. In most of these cases, it is possible to suggest a set of frontier molecular orbitals on the fragment ion and the neutral BBr_3 that can overlap in the initial stage of adduct formation. Computational analysis of transition states for these reactions is required before these suggestions can be substantiated.

The formation of ions containing more than one B atom and/or more than three Br atoms is only predicted computationally at this point and needs experimental verification. This can come in at least two ways. One way is to probe the clusters themselves by examining their dissociation behavior. Measurements of energy thresholds for BBr_3 elimination from clusters would be particularly useful, and high thresholds for such elimination from the small cluster ions that are predicted to be covalently bound would support the computational results. A second means of testing the theoretical predictions would be to investigate reactions between neutral BBr_3 molecules and each of the fragment ions formed in electron ionization of BBr_3.

Acknowledgment. This work was supported by the National Science Foundation (CHE-0212586, CHE-9505444) and Hendrix College. We also are grateful for helpful comments from a reviewer.

Supporting Information Available: Seventeen files containing coordinate tables for all optimized geometries and structures in Protein Data Bank format. This material is available free of charge via the Internet at http://pubs.acs.org.

References and Notes

(1) Massey, A. G. *Adv. Inorg. Chem. Radiochem.* **1983**, *26*, 1−54.
(2) Chiavarino, B.; Crestoni, M. E.; Fornarini, S. *Adv. Mass Spectrom.* **1998**, *14*, A016500/1−A016500/12. Cipollini, R.; Crestoni, M. E.; Fornarini, S. *J. Am. Chem. Soc.* **1997**, *119*, 9499−9503.
(3) Pierce, R. C.; Porter, R. F. *Inorg. Chem.* **1975**, *14*, 1087−1093.
(4) DeLeon, R. L.; Dufresne, C. P.; Rexer, E. F.; Garvey, J. F. *Int. J. Mass Spectrom.* **1999**, *185*−*187*, 149−154.
(5) Overzet, L. J.; Luo, L. *Appl. Phys. Lett.* **1991**, *59*, 161−163.
(6) Jiao, C. Q.; Nagpal, R.; Haaland, P. *Chem. Phys. Lett.* **1997**, *265*, 239−243.
(7) Ring, S.; Eisenhardt, C. G.; Baumgärtel, H. *Chem. Phys. Lett.* **1997**, *280*, 251−259.
(8) Hales, D. A.; Haile, P. A.; Barker, M. P.; Hunt, H. L. *J. Phys. Chem. A* **1998**, *102*, 8305−8311.
(9) Wiley, W. C.; McLaren, I. H. *Rev. Sci. Instrum.* **1955**, *26*, 1150−1157.
(10) BBr_3 vapor pressure calculated using the Antoine equation with parameters from: *NIST Chemistry WebBook, NIST Standard Reference Database Number 69*; Linstrom, P. J., Mallard, W. G., Eds.; National Institute of Standards and Technology: Gaithersburg, MD, Jun 2005 (available at http://webbook.nist.gov).
(11) Koski, W. S.; Kaufman, J. J.; Pachucki, C. F.; *J. Am. Chem. Soc*. **1959**, *81*, 1326−1331.
(12) *Spartan '04* and *Spartan '06*; Wavefunction Inc.: Irvine, CA, 2004 and 2006.
(13) Chase, M. W., Jr. NIST−JANAF Themochemical Tables, Fourth Edition. *J. Phys. Chem. Ref. Data* **1998**, Monograph 9.
(14) IP(B), IP(Br): Lias, S. G. Ionization Energy Evaluation. In *NIST Chemistry WebBook, NIST Standard Reference Database Number 69*; Linstrom, P. J., Mallard, W. G., Eds.; National Institute of Standards and Technology: Gaithersburg, MD, Jun 2004 (available at http://webbook.nist.gov). IP(BBr): ref 11. IP(BBr_3): Bassett, P. J.; Lloyd, D. R. *J. Chem. Soc*. **1971**, (A), 1551−1559.
(15) Lias, S. G.; Bartmess, J. E.; Liebman, J. F.; Holmes, J. L.; Levin, R. D.; Mallard, W. G. *J. Phys. Chem. Ref. Data* **1988**, *17* (Suppl. No. 1), 8.
(16) Deb, B. M. *J. Am. Chem. Soc.* **1974**, *96*, 2030−2044.
(17) Peterson, K. A.; Flowers, B. A.; Francisco, J. S. *J. Chem. Phys.* **2001**, *115*, 7513−7521.
(18) Kim, G.-S.; Hirst, D. M. *Mol. Phys.* **1997**, *90*, 43−47.
(19) Ming, R.; Tao, G.; Ping, H. *Chin. J. Chem. Phys.* **2004**, *17*, 28−32.
(20) Kutz, N. A.; Morrison, J. A. *Inorg. Chem.* **1980**, *19*, 3295−3299.
(21) Farber, M.; Srivastava, R. D. *J. Chem. Phys.* **1984**, *81*, 241.
(22) Ralchenko, Yu.; Jou, F.-C.; Kelleher, D. E.; Kramida, A. E.; Musgrove, A.; Reader, J.; Wiese, W. L.; Olsen, K. *NIST Atomic Spectra Database*, version 3.0.3; National Institute of Standards and Technology: Gaithersburg, MD, 2005; available online at http://physics.nist.gov/asd3 (accessed Jun 2006).
(23) Chase, M. W., Jr.; Davies, C. A.; Downey, J. R., Jr.; Frurip, D. J.; McDonald, R. A.; Syverud, A. N. *J. Phys. Chem. Ref. Data* **1985**, *14* (Suppl. No. 1), 193.
(24) Levine, R. D.; Bernstein, R. B. *Molecular Reaction Dynamics and Chemical Reactivity*; Oxford University Press: New York, 1987; pp 102−103.